Metrol. Meas. Syst., Vol. XVIII (2011), No. 4, pp. 679-690

PAN POLSKA AKADEMIA NAUK

METROLOGY AND MEASUREMENT SYSTEMS

Index 330930, ISSN 0860–8229

www.metrology.pg.gda.pl

M&MS

MEASUREMENT OF THERMAL BEHAVIOR OF DETECTOR ARRAY SURFACE WITH THE USE OF MICROSCOPIC THERMAL CAMERA

Grzegorz Bieszczad, Mariusz Kastek

Military University of Technology, Institute of Optoelectronics, gen. Sylwestra Kaliskiego 2, 00-908 Warsaw, Poland
(✉gbieszczad@wat.edu.pl, +48 22 68 37 55)

Abstract

Modern infrared cameras are constructed with two main types of infrared detectors: photon detectors and thermal detectors. Because of economic reasons, vast numbers of modern thermal cameras are constructed with the use of infrared microbolometric detectors which belong to the group of thermal detectors. Thermal detectors detect incident infrared radiation by measuring changes of temperature on the surface of a special micro-bridge structure. Thermal detectors, like microbolometric detectors on one hand should be sensitive to changing temperature to accurately measure incoming infrared radiation from the observed scene, on the other hand there are many other phenomena that change the temperature of the detector and influence the overall response of the detector. In order to construct an accurate infrared camera, there is a need to evaluate these phenomena and quantify their influence. In the article the phenomenon of self heating due to the operation of the readout circuit is analyzed on an UL 03 19 1 detector. The theoretical analysis is compared with the results of conducted measurements. Measurements with a type SC7900VL thermographic camera were performed to measure the thermodynamic behavior of the UL 03 19 1 detector array.

Keywords: thermovision, microbolometer focal plane array, self heating, microscopic thermography.

© 2011 Polish Academy of Sciences. All rights reserved

1. Introduction

A microbolometer is an infra-red radiation detector which belongs to the thermal sensor family [1-3]. Thermal sensors like microbolometric detectors, absorbs radiation on their surface, causing changes in their temperature. A change of temperature adequate to the amount of absorbed energy causes a change of microbolometer resistance. A specialized readout circuit transforms this resistance change to a voltage signal. Microbolometric detectors have an advantage over photon detectors that they can operate without cryogenic cooling. That is the reason they are called uncooled detectors.

In thermal imaging, microbolometers organized in arrays called focal plane arrays (FPA) are used. An advantage of array of microbolometers is that they can measure the distribution of infrared radiation on an observed scene without any mechanical scanning system. Example pictures of integrated microbolometer arrays are shown in Fig. 1.

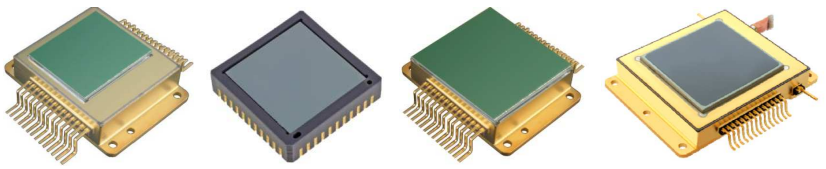

Fig. 1. Examples of microbolometer array packaging.

Article history: received on July 18, 2011; accepted on Nov. 14, 2011; available online on Dec. 12, 2011.

In Europe, the ULIS company (France) produces microbolometric focal plane arrays for the long-wave infrared (8 – 12 μm) spectrum [4]. These detector arrays are manufactured in a CMOS process and are integrated with a readout circuit. Microbolometric detectors have the form of resistive micro-bridges made from amorphous silicon. The characteristic size of a detector depends on the model of the detector array and varies from 35 μm by 35 μm to 17 μm by 17 μm [5-7]. Typical ULIS microbolometric arrays have the thermal resolution defined by noise equivalent temperature difference (NETD) equal to 40 mK when operating in an ambient temperature of 300 K, with an optical system with the aperture 1.0 / F and frame refresh rate of 60 Hz. The microbolometric arrays like the ULIS detectors have a special readout circuit allowing to measure the signal on each detector in the array. The readout circuit is responsible for measuring signals from consecutive detectors by multiplexing them to an integrating amplifier. The integrating amplifier is measuring the current flowing through an active bolometer which is dependent on detector self-temperature. The temperature of the microbolometric detector used in the thermal camera is proportional to the temperature of the observed object in the scene, but also from other sources like camera body or detector substrate. To compensate the influence of detector self-temperature, the signal from the detector is compared with the signal from a so-called blind bolometer which is immune to infrared radiation from the scene. This set of elements constitutes the principal readout circuit for the microbolometric array. The schematic connection between these elements is shown in Fig. 2.

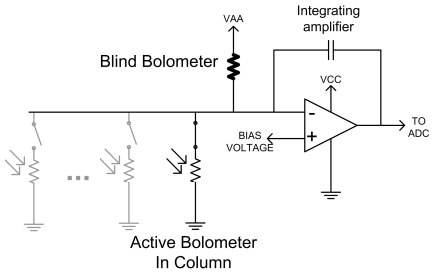

Fig. 2. Microbolometer readout circuit with compensating blind bolometer shown.

To increase the readout speed from the microbolometer array, the readout circuit containing an integrating amplifier and blind bolometer is replicated and connected individually to every column in the array. This makes it possible to integrate all detectors in a row simultaneously. During infrared array operation the readout circuit multiplexes active bolometers from successive rows to the readout circuit. During readout from the detector a small amount of current is flowing through the blind bolometer and active bolometer. A faint difference between currents flowing through the active and the blind bolometer is measured in a transimpedance integrating amplifier and is treated as an useful signal.

2. Thermal properties of the microscopic microbolometric infrared detector

The operating principle of the microbolometric detector is shown schematically in Fig. 3. The infrared radiation incoming to the infrared detector is absorbed on a specially prepared absorber surface. The infrared energy absorbed by the detector is converted to heat. Changes of heat can be measured by the measurement of resistance of the detector which is constructed from a temperature-dependent material – in the measured case amorphous silicon.

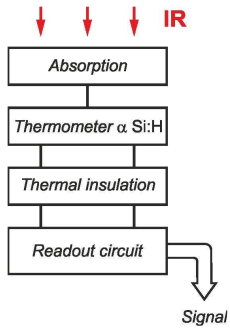

Fig. 3. Microbolometer readout circuit with compensating blind bolometer shown.

The detector is placed on thin supporting leads which have two purposes. First of all they are electrical connectors to the readout circuit, secondly they form a thermal insulation between the detector and rest elements of the detector. Some elements of the readout circuit (ROIC) are made in a CMOS process and placed under the detectors. The ROIC is responsible for converting the detector temperature to a voltage. The schematic picture of the microbolometer structure is presented in Fig. 4.

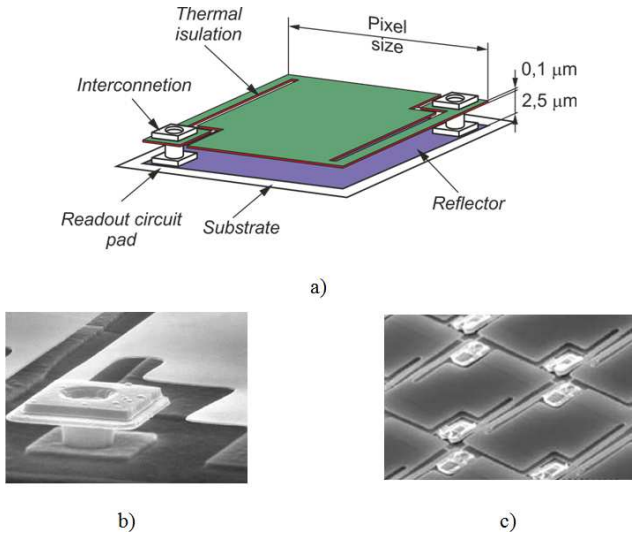

Fig. 4. Example of the microbolometer structure and dimensions a). scanning electron microscope photography of the microbolometer array b), c).

Detectors are enclosed in a hermetic vacuum package with an infrared transparent window on the front side where the special optical lens system is attached to a typical thermal camera.

In order to make a good infrared detector based on microbolometric technology, besides electrical properties like thermal coefficient of the electrical resistance and optical properties like high emissivity coefficient of its surface, it has to have appropriate thermodynamic parameters like thermal resistance and thermal capacity. The thermal resistance of the detector resulting from conductance and convection should be as high as possible to maximize contribution of radiant exchange of energy in the thermodynamic configuration of the detector. The convection thermal resistance of the detector can be maximized relatively easily by placing the detector in vacuum what is done in the case of the detector array we have

investigated. High conductive thermal resistance is achieved thanks to long leads supporting the detector. The producer of the investigated array specifies the thermal resistances of detectors according to the technological process used. Examples of thermal resistances of detectors are shown in Table 1 [8].

Table 1. The coordinates of the absorption peaks in the data representative of the red wine spectrum.

PIXEL PITCH	MINIMUM DESIGN RULE	THERMAL ISULATION R_t
45 μm	1.5 μm	14 MK·W^{-1}
35 μm	1.2 μm	32 MK·W^{-1}
25 μm	0.8 μm	55 MK·W^{-1}

Except the crucial thermal insulation parameter, the second key point to be considered is the pixel time constant. Thermal time constant is an important factor when the thermal camera has to observe dynamic processes. Although this characteristic mainly depends on the application, the typical frame rate of a thermal camera is above 30 Hz. It is commonly admitted that the pixel response time should not exceed one-third of the frame time, in other words, about 10 ms for an array operating at 30 Hz. The pixel thermal time constant depends on its thermal capacity according to the well-known formula

$$\tau = R_t C_t . \tag{1}$$

The thermal capacitance of the detector can be easily calculated knowing all dimensions of the active part of the detector and the specific heat capacity of the material which the detector is made of – in this case amorphous silicon. The thermal capacity of a single detector is approximately:

$$C_t = d \cdot x \cdot y \cdot \rho \cdot c_{a-Si} , \tag{2}$$

where:
d – thickness of the detector – in this case 0.1 μm, x, y – horizontal and vertical dimensions of the detector – in this case 25 μm, ρ – density of silicon – in this case 2329.6 kg/m^3, c_{a-Si} – specific heat capacity of silicon – in this case 705 J/kg·K.

For the case of the detector in the UL 03 16 2 device which has the organization of detectors in an array of 384 x 288 and pixel size of 25 μm and is made with the 0.8 μm design rule, the heat capacity is equal to:

$$C_t = 1{,}02 \cdot 10\text{-}10 \; J/K. \tag{3}$$

Combining this result with thermal isolation for 25 μm pixel size and the minimum design rule 0.8 μm gives a thermal time constant of the detector equal to:

$$\tau = 5{,}64564 \cdot 10^{-3} = 5{,}6 \; ms. \tag{4}$$

This value is similar to 6 ms given by ULIS for this detector type. Other detector types have different time constants due to differences in the technological process. For example the microbolometric detector type UL 03 19 01 has the specified thermal time constant lower than 10 ms and typically 9.5 ms. Differences between these detectors having the same detector size are due to an enhancement in the technological process causing an improvement to 0.5 μm design rule which increased the thermal resistance of the detector [9].

The thermal capacitance of the detector is crucial to detector speed, but also, as will be shown later, to additional thermodynamic effects during detector readout. That motivates to measure the thermal behavior of the detector during readout.

3. Measurement of thermal properties of a microbolometric infrared detector

3.1. Microbolometric array test circuit

A thermal bolometric detector can be used to measure the incident radiation by sensing the detector resistance. In order to properly operate with the array there is the need to set up several biasing voltages necessary for the readout circuit and provide synchronization and control signals. Analog and digital signals were provided thanks to specially developed printed circuit boards, one for a general purpose power supply, a second providing analog biasing signals and a third for digital control. The picture of the electronic circuit with an infrared detector is shown in Fig. 5. An analog circuit board was used to set chosen biasing voltages and changing them during detector operation. A digital circuit board was responsible for generation of a synchronization signal and was able to change several timing parameters of the array during operation, like integration time or frame rate.

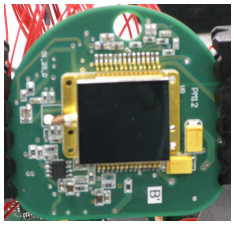

Fig. 5. Printed circuit board of microbolometer array proximity electronics.

When all analog signals are in proper range and the digital circuit produces appropriate synchronization and control signals, the array is ready for readout. The internal readout circuit measures the resistance of the detector and provides the measured value on an analog output pin which is then connected to an ADC converter in the system. In the examined detector array, the resistance of the detectors is internally obtained by measuring the current flowing through them. The current flowing through the detector is being forced by a special biasing voltage called $V_{Skimming}$. For purposes of thermodynamic evaluation of the detector it could be useful to know the exact power provided to the detector during readout. To do so we can use the producer specification of the overall current flowing through the $V_{Skimming}$ circuit or measure it in our circuit. In this type of the detector, the readout of all detectors in a row is made simultaneously thanks to the multiplied integration amplifier circuit common to detectors in every column. This means that during integration time of the signal from the detector, the current flows through every detector in a currently read row. When all signals in a row are integrated, the multiplexing circuit switches to the next row in the array and the process repeats. The relatively low amount of current flowing through the detector during integration causes a considerable increase of detector temperature due to the voltage drop across its resistance. The power delivered to the detector during readout causes a systematic error added to the signal from the detector. Additionally the power delivered to the detector changes with readout circuit integration time and biasing voltage level, causing a variation of the additional error signal. The behavior of this phenomenon was evaluated on a specially designed measurement stand.

3.2. Measurement stand

In order to perform a measurement of the microbolometer temperature change phenomenon, a special measurement setup was designed, allowing experimentation on the microbolometer detector array with variable timing parameters like frame readout frequency or integration time. Thanks to the infrared camera used there was a possibility to precisely match the camera's frame rate to the readout frequency of the microbolometer array. The scheme of the measurement stand is shown in Fig. 6a. The main component of the measurement stand consists of a type SC7900VL infrared camera and attached microscopic infrared lens. The infrared camera in setup with infrared detector is shown in Fig. 6b.

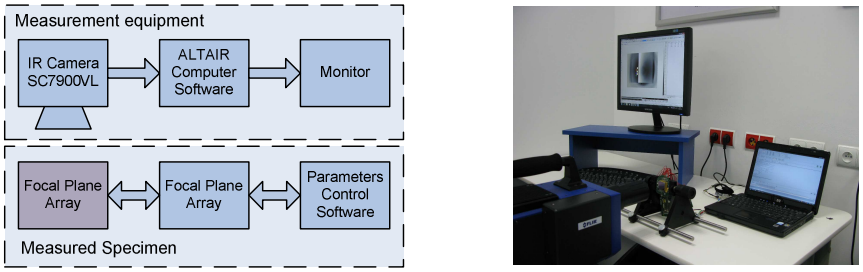

a) b)

Fig. 6. Measurements stand for microbolometric array evaluation: block diagram (a) and real setup (b).

The chosen infrared camera works in the long-wave infrared (LWIR) spectral range. The measured infrared detector is enclosed in a vacuum package and it receives infrared radiation through an infrared transparent window made from germanium. The germanium window is designed to be transparent to infrared radiation in the 8 μm to 14 μm spectral range. This means that the spectral range of the thermal camera is detecting infrared radiation within the window transparent range. Thanks to the matched infrared spectral range there is the possibility to minimize errors due to selective emission of detector's opening window and attenuation of radiation in the window.

The infrared camera type SC7900VL from Flir Systems is equipped with a MCT detector array with 320 x 256 detectors. The camera offers the possibility of continuous registration or on a frame-by-frame basis. The camera provides a thermal resolution NETD equal to 25 mK, and measures infrared radiation in the spectral range of 7.7 to 11.5 μm. During measurement the camera was equipped with microscopic lens providing 3x magnification. The minimal observation area for this lens is 3.20 by 2.56 mm. The observed area can be expanded to the values determined by measured specimen size. The measured active area of the detector has a size of 9.6 x 7.2 mm.

Thanks to the AltaIR software provided with the camera for command and control purposes, there is a possibility to change the camera's operating parameters like frame rate, integration time, and also parameters regarding the measured object like its emissivity coefficient, atmospheric transmission and ambient temperature. All these parameters have an impact on resulting measurement values. From all these parameters the greatest influence on measurement accuracy has the emissivity coefficient [10]. In order to eliminate the impact of changes in emissivity factor when measuring an object or uncertainty in estimation of the real value of emissivity, various techniques are used [11, 12]. Using the SC7900VL camera there, it is possible to define and introduce the emissivity map before or after the measurement,

making the measurement independent from its effect on the accuracy of the temperature distribution.

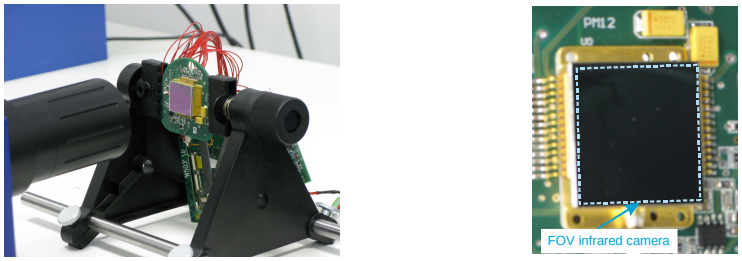

a) b)

Fig. 7. The close-up on the measured device (a), SC7900VL infrared camera field of view (b).

The distance between the measured specimen and the camera was small enough to neglect the impact of air transmission. The photograph of the measurement setup is shown in Fig. 7a. The infrared camera with close-up optical lens was able to cover the whole infrared array with its field of view as shown in Fig. 7b. The attenuation effect of the germanium glass cover was taken into account with an assumed τ_{wm} = 0.8 transmission coefficient. That value was provided by the producer of the detector. The emissivity of the detector surface was also provided by the producer (ULIS) and was equal to 0.8. When measuring temperature and humidity they were monitored by the meter and put into software before each measurement.

The SC7900VL thermovision camera allows setting the frame rate and active field of view for a measurement. The frame rate can be set from 2 Hz to 235 Hz in the full frame mode. The active frame can be set to almost any size below the array size of 320 x 256 detectors. During the measurement, full frame acquisition was used with different frame rates matched to the examined specimen operation frequency.

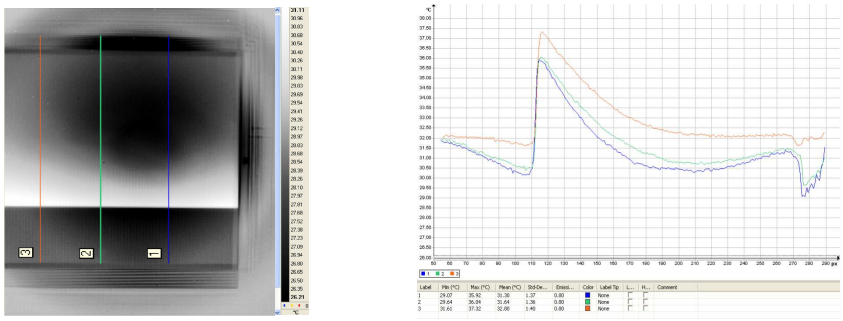

a) b)

Fig. 8. Thermogram registered during the measurement (a), temperature change on profiles (b).

The registered thermograms were analyzed with AltaIR software by evaluating single frames and the whole sets of image sequences. The software allows analysis of temperature changes in space and time along the specified profile and statistical properties of its distribution. In Fig. 8a a registered thermogram of microbolometric array during operation with an integration time of 104 μs is shown. For analysis, three columns were chosen to show

the distribution of temperature. The distribution of temperature along profiles is shown in Fig. 8b. Additionally, radiometric data was exported and analyzed in Matlab software.

3.3. Thermodynamic model of detector

Having in mind all previous considerations, a simplified thermodynamic model of the detector was elaborated. The picture of model elements is shown in Fig. 9.

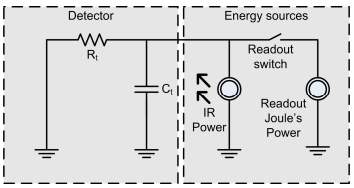

Fig. 9. Thermodynamic model of a single detector in array.

The detector is characterized by its thermal capacity and its thermal resistance to the substrate of the detector which are at ambient temperature. The detector is exposed to infrared radiation which affects its temperature. Additionally during integration time the detector is receiving additional energy from the readout circuit. Additional energy from the readout circuit is provided periodically for a very short time proportional to the integration time. This energy impulse is provided directly to the detector through flowing current and is being stored in detector's thermal capacitance. After readout the additional energy in the detector decays due to thermal resistance to the detector substrate.

The theoretical increase of temperature was estimated according to the formula:

$$\Delta T = \frac{P_{read-out}}{C_t} = \frac{I^2 \cdot R_{\mathrm{det}} \cdot t_{\mathrm{int}}}{C_t}, \tag{5}$$

where:

$P_{read-out}$ – additional Joule power provided during the readout phase, I – current flowing through the single detector during readout, R_{det} – electrical resistance of the detector, t_{int} – is the integration time of a pixel in the row, C_t – detector thermal capacitance estimated earlier.

The numerator in equation 5 is the energy delivered to the detector during readout, while the denominator is the thermal capacitance where the energy was stored. The thermal time constant of the detector can be here neglected, because integration time is much lower than the detector time constant. The energy received due to the measurement current caused a rapid increase of temperatures which then decays according to the thermal time constant. The theoretical increase of temperatures for type UL 03 19 01 detector and integration times from 20 µs to 104 µs can be between 1ºC to 7ºC. The thermal behavior (not to scale) of the detector is shown in Fig. 10.

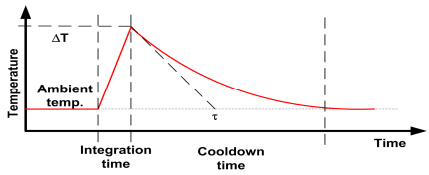

Fig. 10. Theoretical thermal behavior of the detector.

3.4. Data analysis

There are several ways to evaluate thermal properties like thermal time constant of the detector with thermal camera. For example, we can measure the surface temperature of the detector with precise timestamp and with high frame rate sufficient to sample the detector temperature several times during its decay time. On the other hand we can make a measurement and exploit the knowledge about timing specification of the readout circuit. We know that every consecutive row in this setup is read with 9.2 kHz frequency, giving a time between every row readout of about 108 μs. Knowing the time which elapsed from readout for every row in an array and assuming identical thermal behavior of every detector in the array, there is a possibility to take a whole temperature profile of the detector with one snapshot of the thermal camera. Evaluating the temperature profile across a chosen column of detectors there is a possibility to quantify the temperature decay with a time resolution equal to the time between row readout which gives a 108 μs time resolution. To achieve this with the first method we would need a 9.2 kHz camera frame rate. In some cameras the frame rate is limited and it is impossible to measure fast processes, but with methodology applied to this measurement we can achieve better results with just one thermal image snapshot.

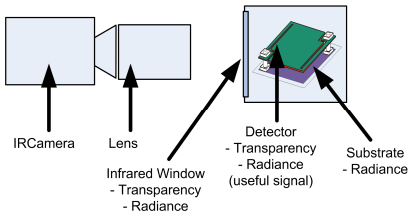

Fig. 11. Measurement stand schematic and parameters affecting the measured results.

There are several properties of investigated specimen that affect the temperature measurement reading of the thermal camera. A diagram of the measurement stand and origin of some phenomena affecting the measurement is shown in Fig. 11. The phenomena that have to be taken into account in this measurement setup are:

- lens radiometric properties;
- infrared window transparency coefficient;
- infrared window radiation;
- detector fill factor which is equal to 70%;
- detector emissivity coefficient and its transparency;
- radiance of the substrate.

Part of the measurement correction due to the measurement setup can be taken into account in thermal camera software, but some has to be calculated offline. Infrared camera software was used to recalculate radiometric data to temperature with corrections to IR camera lens, infrared window transparency and emissivity of the detector. The IR camera was configured to cooperate with microscopic lens and a standard calibration procedure was applied. In the measurement setup the emissivity coefficient was set to 0.8 which is a typical value for modern microbolometer detectors [13, 14].

Measurement was performed for different integration times, which allowed to control the amount of energy injected to the microbolometer bridge during readout. Examples of measured thermograms for different integration times are shown in Fig. 12.

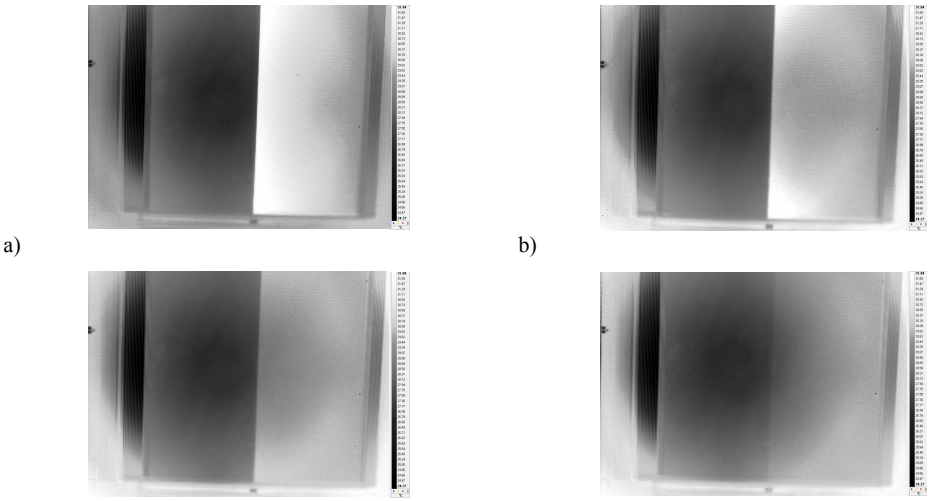

Fig. 12. Measured thermograms of detector array surface for different integration times: 81 μs (a), 54 μs (b), 27 μs (c) and 4.3 μs (d).

Unfortunately, even with the microscopic camera used, the spatial resolution of the camera was insufficient to precisely measure the temperature of the detector surface. The area measured by a single detector was a little bit bigger than the size of the detector. That means that the camera was sensing the averaged equivalent temperature of the detector and other elements like supporting leads and substrate. Knowing the ratio between the detector area and substrate area and the substrate temperature, there is a possibility to calculate detector temperature. The ratio between detector area and substrate area is called the fill factor and is characteristic to a given detector type and provided by the producer of the detector. For example, the measured detector array has a fill factor of about A_{ff}=0.7. The correction to the detector fill factor affecting the mean measured temperature was introduced in post processing. Fill factor correction was introduced to the captured thermogram in the camera according to the formula (6).

$$T_{\text{det}} = A_{ff} T + \left(1 - A_{ff}\right) T_{substrate}, \tag{6}$$

where:

A_{ff} – is an area fill factor, $T_{substrate}$ – is the temperature of the silicon substrate the detector is attached to, T – is the temperature determined from the thermogram.

This correction is valid with linear temperature share approximation to emitted energy, which is valid only for small temperature differences. The result of analysis was shown in recalculated thermogram of the structure with all mentioned phenomena taken into account in Fig. 12.

Knowing the time between each row readout, there is a possibility to calculate the time between readout and infrared image snapshot for every observed detector. Assuming the same thermal behavior of all detectors in the examined array, one can create a dataset of time-stamped temperature readings associated with detector temperature in the chosen column of detectors, where a number of each row in the detector corresponds to calculated time from beginning of integration. An exemplary graph of temperature of the detector in time is shown in Fig. 13.

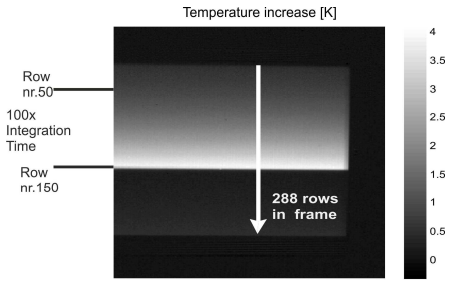

Fig. 13. Processed thermogram of temperature increase for integration time equal to 54 µs.

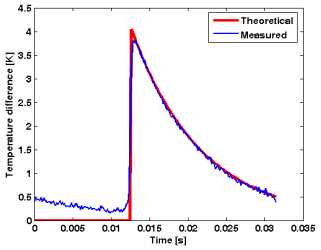

Fig. 14. Measured temperature profile compared with matching theoretical profile.

This result was compared with theoretical temperature behavior of the single detector described earlier. The time constant of the detector was established using least square matching of theoretical temperature decay and the measured one. A measured and matched theoretical curve is shown in Fig. 14. All evaluated thermal parameters of detector are presented in Table 2 and compared with theoretical values. Measurement of temperature increase was performed for multiple integration times.

Table 2. Theoretical and measured thermodynamic parameters of the detector.

INTEGRATION TIME	MEASURED TEMPERATURE DIFFERENCE	THEORETICAL TEMPERATURE DIFFERENCE	MEASURED THERMAL TIME CONSTANT
104 µs	6.3 °C	8.2 °C	8.5 ms
81 µs	6.2 °C	6.4 °C	8.5 ms
54 µs	3.3 °C	4.3 °C	8.5 ms
27 µs	1.5 °C	2.1 °C	8.5 ms
4.3 µs	0.1 °C	0.3 °C	8.5 ms

4. Conclusions

Measurement of thermodynamic parameters allows to evaluate modern infrared detectors in terms of their characteristics directly affecting their performance. Evaluation of the self-heating phenomenon opens the possibility to develop algorithms to compensate its effects. Many research institutes developing infrared array readout circuits are working on algorithms and techniques to compensate the self-heating phenomenon effects on sensitivity and accuracy of an infrared detector. Some of these methods are made in software, but sometimes as presented [15] they involve hardware changes in the detector structure, for example by

adding an additional bimorph leg. A software solution to compensate the self-heating phenomenon will be elaborated in future.

Acknowledgements

Scientific work funded from the Science Fund for years 2009-2011 as a development project.

References

[1] Tissot, J.L., Trouilleau, C., Fieque, B., Crastes, A., Legras, O. (2006). Uncooled microbolometer detector: recent developments at ULIS. *Opto-Electron Review,* 14(1), 25-32.

[2] Bieszczad, G., Orżanowski, T., Sosnowski, T., Kastek, M. (2009). Method of detectors offset correction in thermovision camera with uncooled microbolometric focal plane array, *Proc. of SPIE*, 7481, 74810O.

[3] Orżanowski, T., Madura, H. (2009). Test and evaluation of reference-based nonuniformity correction methods for microbolometer infrared detectors. *Opto-electronics Review*, 18 (1), 91-94.

[4] Trouilleau, C., Crastes, A., Fièque, B., Legras, O., Tissot, J.L. (2005). Uncooled microbolometer detector: recent developments at ULIS. *Proc. of SPIE*, 5978, 597815.

[5] Tissot, J.L., Fieque, B., Trouilleau, C., Robert, P., Crastes, A., Minassian, C., Legras, O. (2006). First demonstration of 640x480 uncooled amorphous silicon IRFPA with 25 µm pixel-pitch, *Proc. of SPIE*, 6206, 620618.

[6] Trouilleau, C., Crastes, A., Legras, O., Tissot, J.L., Chatard, J.P. (2005). 35 µm pitch at ULIS, a breakthrough. *Proc. of SPIE*, 5783, 578-585.

[7] Mendel, C., Martin, J.L., Ouvrier-Buffet, J.L., Tissot, J.L., Vilain, M., Yon, J.J. (1999). Amorphous silicon based uncooled microbolometer IRFPA. *Proc. of SPIE*, 3698, 276-283.

[8] Yon, J.J., Mottin, E., Tissot, J.L. (2008). Latest amorphous silicon microbolometer developments at LETI-LIR. *Proc. of SPIE*, 6940, 69401W.

[9] Crastes, A., Tissot, J.L., Vilain, M., Legras, O., Tinnes, S., Minassian, C., Robert, P., Fieque, B. (2008). Uncooled amorphous silicon ¼ VGA IRFPA with 25 µm pixel-pitch for high end applications. *Proc. of SPIE,* 6940, 69401V.

[10] Madura, H., Kastek, M., Sosnowski, T., Orżanowski, T. (2010). Pyrometric method of temperature measurement with compensation for solar radiation. *Metrology and Measurement Systems*, 17(1), 77-86.

[11] Madura, H., Kastek, M., Piątkowski, T. (2007). Automatic compensation of emissivity in three-wavelength pyrometers. *Infrared Physics & Technology*, 51(1), 1-8.

[12] Bielecki, Z., Chrzanowski, K., Matyszkiel, R., Piątkowski, T., Szulim, M. (1999). Infrared pyrometer for temperature measurement of objects of both wavelength- and time-dependent emissivity. *Optica Applicata*, 29(3), 284-292.

[13] Misook, Ahn, Yong-Hee, Han, Sung, Moon. (2007). A novel infrared absorbing structure for uncooled infrared detector. *Current Applied Physics*, 7(6), 617-621.

[14] Hwang, C.H., Lee, Y.S., Lee, H.L. (2006). High-Performance Pixelwise Readout Integrated Circuits for Microbolometer. *Proc of Electronics, Circuits and Systems*, ICECS '06. 13th, 1140-1143.

[15] Jo, Y., Kwon, I.L., Kim, D.S., Shim, H.B., Lee, H.C. (2011). A self-protecting uncooled microbolometer structure for uncooled microbolometer. *Proc. of SPIE*, 8012, 80121O.